

- the reaction, its ability to operate at ~50% efficiency at 0.02 mol% of substrate and the fact that cholesterol has been measured at 6% by weight of total lipid in the endoplasmic reticulum of eukaryotic cells [B. Alberts, *et al.*, *Molecular Biology of the Cell* (Garland, New York, ed. 3, 1994)] suggests a physiologically relevant affinity of His₆-Hh-C for cholesterol.
17. M. L. Cardoso de Almeida and M. J. Turner, *Nature* **302**, 349 (1983).
 18. Metabolic labeling of S2 cultured cells with [³H]cholesterol was done essentially as described (28). Briefly, cells containing a stably integrated Cu²⁺-inducible *hedgehog* gene were grown at 23°C for 2 weeks in Schneider cell media (Gibco) containing 5% fetal bovine serum depleted of lipoprotein (low-cholesterol media, ~20 μg of cholesterol per milliliter). These cells were then plated at 40% confluence onto two 35-mm tissue culture dishes (Nunc) in 1 ml of low-cholesterol media supplemented with 300 μCi of labeled cholesterol [1,2,6,7-³H (N)] (65 Ci/mmol, NEN) giving a specific activity for cholesterol in this medium of ~5 Ci/mmol. After 24 hours (one doubling time), one plate of cells was induced to express Hh protein by the addition of CuSO₄ (final concentration, 1 mM). After an additional 24 hours, the cells from both dishes were harvested, then lysed in tris-buffered saline containing 1% Triton X-100, and total cell protein was precipitated with 5 volumes of cold acetone. The protein pellet was resuspended in 2% SDS in H₂O and reprecipitated with acetone several times to remove unincorporated radioactivity before loading onto SDS-polyacrylamide gels for analysis. Initial labeling experiments with 25 μCi of added cholesterol resulted in reduced incorporation by a factor of ~10.
 19. HPLC analysis of the Hh-N_p adduct involved gel isolation of the radioactive band, KOH-methanol treatment of the band to break the ester linkage (40), followed by neutralization of the solution with acetic acid, drying in a Speedvac, resuspension in H₂O, and extraction of the hydrophobic radioactivity with ether. After evaporation of the ether, the sample was resuspended in isopropanol and applied to the C18 column for analysis (20).
 20. R. J. Rodriguez and L. W. Parks, *Methods Enzymol.* **111**, 37 (1985).
 21. The specific activity of [³H]cholesterol in the S2 cell labeling medium was ~5 Ci/mmol. Assuming after a 24-hour doubling time that this concentration approximately represents that within the S2 cell membrane, then any protein subsequently expressed and receiving cholesterol as an adduct would also be labeled at the same specific activity. As determined by standardized Coomassie blue staining, ~50 to 100 ng (2.5 to 5 picomol) of Hh-N_p is produced by one 35-mm dish of S2 cells containing the Cu²⁺-inducible Hh construct during 24 hours of induction with 1 mM CuSO₄ (13). This amount predicts that ~12.5 to 25 nCi (2.75 × 10⁴ to 5.5 × 10⁴ dpm) of radioactivity would be incorporated into Hh-N_p protein produced in our labeling experiment, assuming that the protein is cholesterol modified. Total incorporation of radioactivity into Hh-N_p during the *in vivo* labeling experiment described above (18) was measured at ~5 × 10⁴ dpm by excision and scintillation counting of an Hh-N_p gel band.
 22. A recent matrix-assisted laser desorption ionization (MALDI) mass spectral analysis (8) gave a mass of ~430 daltons for the Hh-N_p adduct, ~9% larger than the mass of cholesterol (386.6 daltons). Detection of this modification required that Hh-N_p be treated with cyanogen bromide (CNBr) in 70% formic acid because full-length Hh-N_p could not be detected. The mass discrepancy noted above could be accounted for by the net addition of formic acid (45 daltons) during CNBr digestion. This reaction could involve the addition of H₂O across the 5,6 double bond of cholesterol, a common reaction of secondary alkenes in strong acids [R. T. Morrison and R. N. Boyd, *Organic Chemistry* (Allyn Bacon, Boston, ed. 3, 1973)], followed by esterification of formate via this newly formed alcohol [B. I. Cohen, G. S. Tint, T. Kuramoto, E. H. Mosbach, *Steroids* **25**, 365 (1975)]. To determine whether the sterol backbone could be modified by the CNBr treatment, we examined a positively charged cholesterol derivative (3β-(N,N'-dimethylamino)ethanecarbonyl)-cholesterol (Sigma) detectable by MALDI. Incubation of this sterol derivative in 70% formic acid alone resulted in the addition of 45 mass units to the sterol (13), a mass consistent with the net addition of a formic acid molecule.
 23. COS-7 cells grown at 37°C in Dulbecco's modified Eagle's medium (DMEM) supplemented with 10% fetal calf serum were plated at ~35% confluence onto two 35-mm dishes in 1 ml of Optimem media (Gibco) containing 1.5% fetal bovine sera and 250 μCi of [³H]cholesterol, giving a final concentration of cholesterol of ~40 μg/ml with a specific activity of 2 Ci/mmol (labeling medium). After 24 hours the labeling medium was removed and the cells were transfected for 6 hours with *Shh* or *Shh-N* expression constructs with lipofectamine (Gibco) and serum-free DMEM. After transfection, 1 ml of fresh labeling medium was added to each dish, and the cells were incubated for 36 hours at 37°C. The cells were then harvested without washing and lysed on the plate with tris-buffered saline plus 1% Triton X-100, and the total cell proteins were precipitated with acetone, washed, and analyzed as described above for the S2 cell proteins.
 24. G. F. Gibbons, K. A. Mitropoulos, N. B. Myant, *Biochemistry of Cholesterol* (Elsevier, Amsterdam, 1982).
 25. M. S. Brown and J. L. Goldstein, *Cell* **71**, 187 (1992).
 26. P. L. Yeagle, *Biochim. Biophys. Acta* **822**, 267 (1985).
 27. J. DuPont, *Cholesterol Systems in Insects and Animals* (CRC Press, Boca Raton, FL, 1982).
 28. M. Silberkang, C. M. Havel, D. S. Friend, B. J. McCarthy, J. A. Watson, *J. Biol. Chem.* **258**, 8503 (1983).
 29. J. A. Svoboda and G. F. Weirich, *Lipids* **30**, 263 (1995).
 30. A. J. Forbes, H. Lin, P. W. Ingham, A. C. Spradling, *Development* **122**, 1125 (1996).
 31. C. Roux, *Arch. Fr. Pediatr.* **21**, 451 (1964).
 32. _____, *C. R. Seances Soc. Biol. Fil.* **160**, 1353 (1966).
 33. _____, C. Horvath, R. Dupuis, *Teratology* **19**, 35 (1979).
 34. C. Roux, R. Dupuis, C. Horvath, A. Giroud, *ibid.*, p. 39.
 35. C. Roux *et al.*, paper presented at the 23rd Annual Conference of the European Teratology Society, Dublin, Ireland, 4 to 7 September 1995.
 36. G. Xu *et al.*, *Gastroenterology* **109**, 1301 (1995).
 37. G. S. Tint *et al.*, *N. Engl. J. Med.* **330**, 107 (1994).
 38. J. M. Opitz, *Am. J. Med. Genet.* **50**, 344 (1994).
 39. G. Salen *et al.*, *J. Lipid Res.* **37**, 1169 (1996).
 40. M. C. Field and A. K. Menon, in *Lipid Modification of Proteins*, N. M. Hooper and A. J. Turner, Eds. (Oxford Univ. Press, New York, 1992), p. 155.
 41. We are grateful to A. Woods and D. Raben for use of equipment and for helpful advice. We thank J. Nathans, D. Leahy, and T. Tanaka-Hall for comments on the manuscript. P.A.B. is an Investigator of the Howard Hughes Medical Institute.

2 August 1996; accepted 27 August 1996

Gastric Mucosa Abnormalities and Tumorigenesis in Mice Lacking the pS2 Trefoil Protein

Olivier Lefebvre, Marie-Pierre Chenard, Régis Masson, José Linares, Andrée Dierich, Marianne LeMeur, Corinne Wendling, Catherine Tomasetto, Pierre Chambon, Marie-Christine Rio*

To determine the function of the pS2 trefoil protein, which is normally expressed in the gastric mucosa, the mouse *pS2* (*mpS2*) gene was inactivated. The antral and pyloric gastric mucosa of *mpS2*-null mice was dysfunctional and exhibited severe hyperplasia and dysplasia. All homozygous mutant mice developed antropyloric adenoma, and 30 percent developed multifocal intraepithelial or intramucosal carcinomas. The small intestine was characterized by enlarged villi and an abnormal infiltrate of lymphoid cells. These results indicate that *mpS2* is essential for normal differentiation of the antral and pyloric gastric mucosa and may function as a gastric-specific tumor suppressor gene.

The human (hpS2) (1) and mouse (mpS2) (2) pS2 proteins belong to the family of trefoil peptides, which are characterized by the presence of one to six cysteine-rich P domains (3, 4). Although hpS2 and mpS2 are normally expressed in the gastric mucosa (2, 5), hpS2 is also abnormally expressed

in ulcerative gastrointestinal diseases (6) and in various cancers (7–9). In all cases, hpS2 and mpS2 are found in the cytoplasm of epithelial cells (2, 9). It has been proposed that pS2 functions as a growth factor, a protease inhibitor, or a mucin stabilizer to modulate cell growth and protect the integrity of the gastric mucosa (9, 10). To elucidate the function of pS2, we disrupted the mouse *pS2* gene by homologous recombination.

We cloned and sequenced the *mpS2* gene (11). It encompasses 4.1 kb and contains three exons (Fig. 1A). Exon 1 [96 base pairs (bp)] encodes the NH₂-terminal signal peptide, exon 2 (153 bp) encodes the P domain,

O. Lefebvre, R. Masson, J. Linares, A. Dierich, M. LeMeur, C. Wendling, C. Tomasetto, P. Chambon, M.-C. Rio, Institut de Génétique et de Biologie Moléculaire et Cellulaire, CNRS/INSERM/Université Louis Pasteur/Collège de France, Boite Postale 163, 67404 Illkirch Cedex, Communauté Urbaine de Strasbourg, France. M.-P. Chenard, Service d'Anatomie Pathologique Générale, Centre Hospitalier Universitaire de Hautepierre, 67098 Strasbourg Cedex, France.

*To whom correspondence should be addressed.

and exon 3 (198 bp) encodes the five COOH-terminal amino acids and the 3' untranslated region. To inactivate the *mpS2* gene, we constructed a pRH1-4neo targeting construct encoding 45 *mpS2* amino acids corresponding to the signal peptide and 15 to 20 amino acids of the mature *mpS2*, as well as the neomycin resistance gene (*neo*) (Fig. 1, A and B). pRH1-4neo was electroporated into D3 embryonic stem (ES) cells, and two clones showed a Bam HI DNA restriction pattern consistent with disruption of one of the *mpS2* alleles (Fig. 1C). No additional integrated copies of the targeting construct were detected in these clones when examined with a *neo* probe. One of the clones was microinjected into 300 C57BL/6J blastocysts, which were reimplanted in pseudogestante females. Five chimeric males were generated, and one of them transmitted the mutant allele to offspring when mated with 129/Svj females, yielding *mpS2*^{+/-} heterozygotes. These mice were subsequently mated to yield homozygous *mpS2*^{-/-} mice (Fig. 1D).

Inactivation of the *mpS2* gene was demonstrated by Northern (RNA) blot analysis of total RNA extracted from stomachs of *mpS2*^{+/+}, *mpS2*^{+/-}, and *mpS2*^{-/-} littermates. The 0.6-kb wild-type transcript was seen in the *mpS2*^{+/+} and *mpS2*^{+/-} mice, whereas the 1.8-kb recombinant transcript containing the *neo* sequence was present only in *mpS2*^{+/-} and *mpS2*^{-/-} mice (Fig.

2A). Expression of the *mpS2* protein was investigated by immunoblot analysis of gastric cytosol and immunohistochemistry of stomach samples. The *mpS2*^{+/+} and *mpS2*^{+/-} mice expressed high and intermediate levels of *mpS2*, respectively, whereas the *mpS2*^{-/-} mice showed no detectable expression (Figs. 2B and 3, G and H).

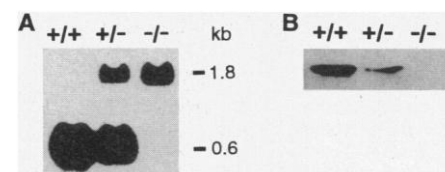
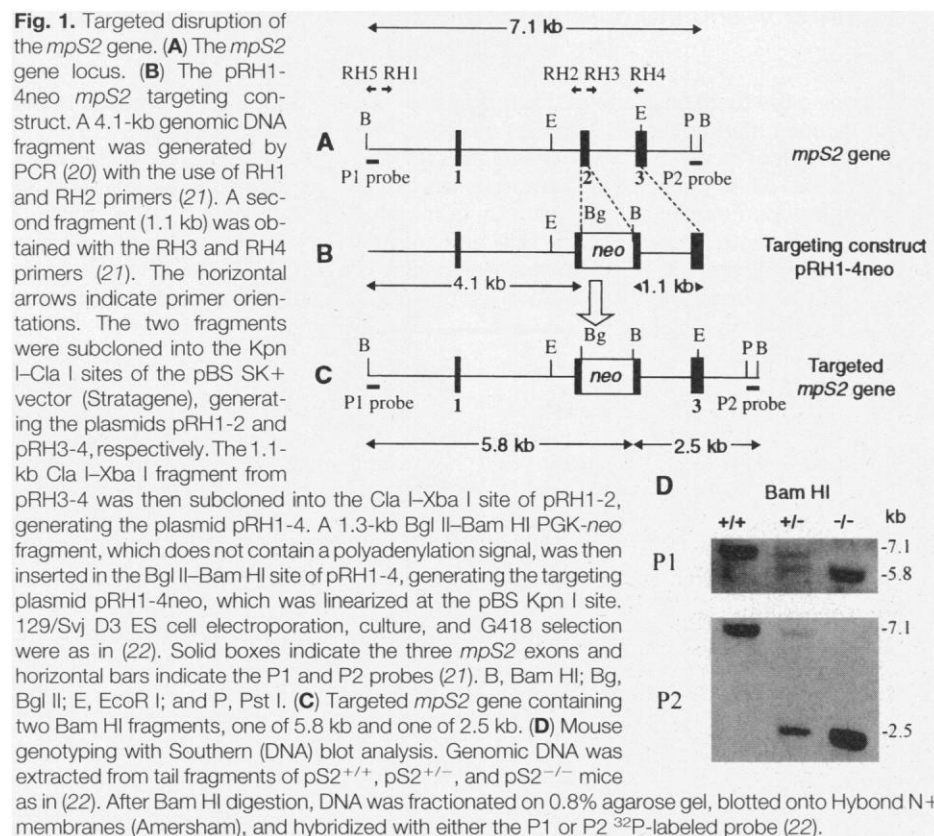
Genotyping of 86 3-week-old offspring from *mpS2*^{+/-} crosses revealed a frequency of 32.5% *mpS2*^{+/+}, 46.5% *mpS2*^{+/-}, and 21% *mpS2*^{-/-} mice. When interbred, the *mpS2*^{-/-} mice were fertile, giving rise to an average of eight pups per litter, which suggests that there was no embryonic lethality. The appearance and behavior of 5-month-old *mpS2*^{+/+} and *mpS2*^{-/-} mice were indistinguishable from those of *mpS2*^{+/+} mice. Histologic examination of the brain, heart, lung, liver, pancreas, spleen, muscle, mammary gland, colon, testis, ovary, uterus and kidney from 10 *mpS2*^{+/+} and 10 *mpS2*^{-/-} mice at 5 months of age did not reveal any obvious differences (12).

In contrast, abnormalities were consistently observed in the stomach and small intestine of the *mpS2*^{-/-} mice (Fig. 3). Whereas the fundus mucosa did not show any obvious abnormality, the antral and pyloric mucosa was thicker in *mpS2*^{-/-} mice. Both sexes were equally affected, and the phenotype was fully penetrant in the 20 *mpS2*^{-/-} mice examined. The mucosa of

3-week-old pups (10 specimens) was already twice the normal thickness (12). At 5 months, all examined *mpS2*^{-/-} mice (10 specimens) exhibited a circumferential adenoma encompassing the whole antropylo-ric mucosa (Fig. 3, A and B). The antral and pyloric mucosa showed severe hyperplasia with markedly elongated pits occupying most of the thickness of the mucosa, whereas the glands had a normal appearance (Fig. 3, C and D). The epithelial cells lining the surface and the elongated pits showed high-grade dysplasia: The nuclei were enlarged and hyperchromatic and showed loss of polarity (Fig. 3, E and F). In addition, the antral and pyloric epithelial cells exhibited a 10-fold increase of the mitotic index (12) and were improperly differentiated and dysfunctional, as they were almost entirely devoid of mucus as shown by periodic acid of Schiff (PAS) staining (Fig. 3, I and J). In the upper part of the adenoma, the glandular architecture was distorted, with some branching and intraglandular bridging (Fig. 3, D, F, H, and J).

Two to five foci of carcinoma were observed within the adenoma in 30% of 5-month-old *mpS2*^{-/-} mice. Glands were irregular and were closely packed together in a "back-to-back" pattern (Fig. 3K), and sheets of epithelial cells that had crossed through the basement membrane could be seen in the lamina propria (LP) (Fig. 3L). These features are characteristic of intraepithelial and intramucosal carcinomas, respectively (13). There was no evidence of metastatic dissemination to the lungs or liver.

At 5 months, the villi of the small intestinal mucosa of *mpS2*^{-/-} mice were enlarged by a thickened LP, whereas the length of the villi was normal (Fig. 3, M through P). Epithelial cells lining the villi were normally differentiated, exhibited the



usual ratio of goblet cells and enterocytes, and stained positively for mucus, which indicates that they were functional (12). The thickened LP contained inflammatory cells, including lymphocytes, plasmocytes, and a few macrophages. The number of intraepithelial lymphocytes (14) was also increased (Fig. 3P). No alterations in the small intestine were observed in 3-week-old *mpS2*^{-/-} mice, which suggests that *mpS2* is not required for small intestine ontogenesis but is required for normal intestinal function later in life. By contrast, the large bowel was never affected. The *pS2* protein, which is resistant to gastrointestinal proteases and has been found in gastric juice (5), may exert a protective function in the small intestine (15), and its absence may lead to small intestine mucosal barrier defects accompanied by a local lymphoproliferative response. Abnormal overexpression of *hpS2* has been observed in human gastrointestinal acute inflammatory disorders such as duode-

nal ulceration and Crohn disease at the time of tissue regeneration, suggesting that *hpS2* could be involved in the protection of gastrointestinal mucosal integrity (6). However, no ulcerations were observed in the small intestine of *mpS2*^{-/-} mice.

In addition to *mpS2*, two other murine trefoil peptides have been identified: *mITF*, which is normally expressed in the intestine and colon (16), and *mSP*, which is expressed in the stomach, duodenum, and pancreas (3). Expression of *mITF* was not affected in the *mpS2*^{-/-} mice. In contrast, *mSP* expression was not detected in the *mpS2*^{-/-} stomach samples but was detected in the *mpS2*^{-/-} pancreas samples (Fig. 4). However, this lack of gastric *mSP* expression was not fully penetrant: Of 16 *mpS2*^{-/-} mice studied, 11 showed an absence of *mSP* mRNA, 2 had normal levels, and 3 had reduced levels. Thus, the gastric mutant phenotype that was fully penetrant in *mpS2*^{-/-} mice can be directly attributed to the absence of the *mpS2* protein. How dis-

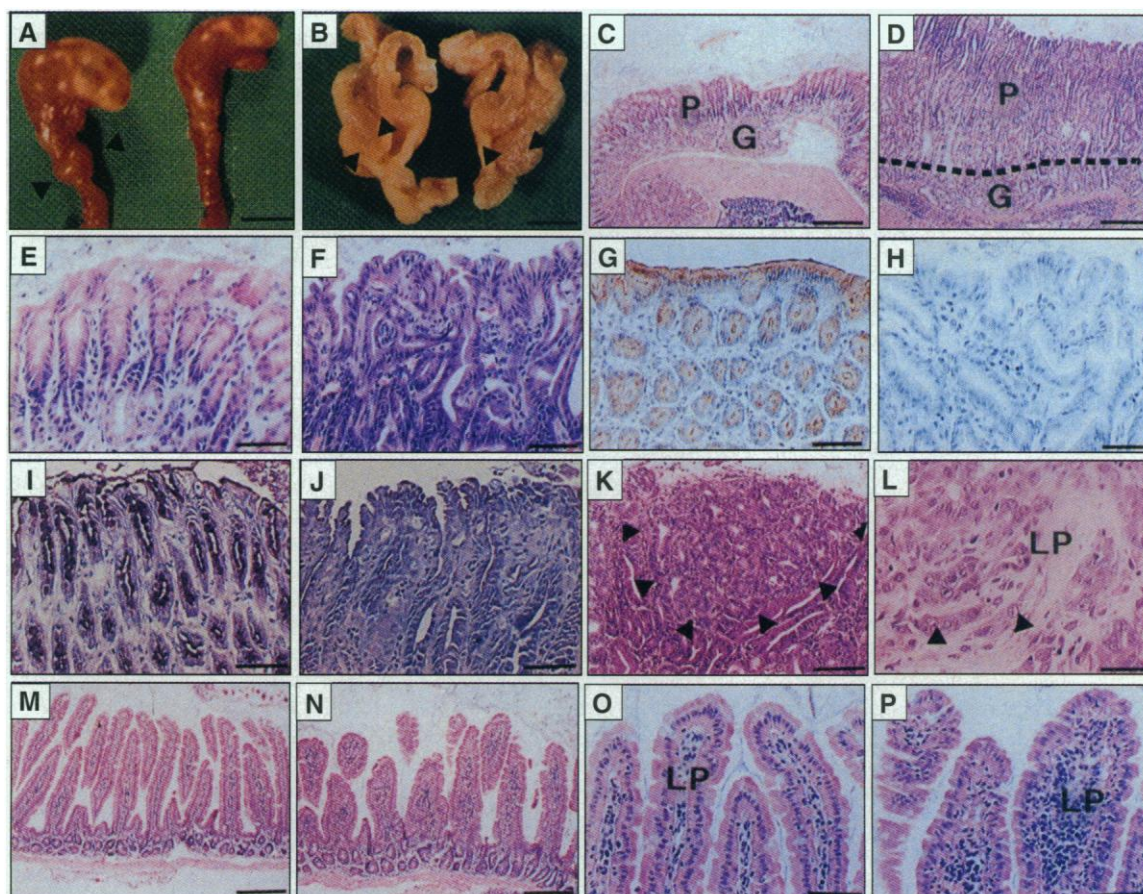
ruption of *mpS2* specifically affects *mSP* expression in the stomach is unknown. The fact that trefoil peptide genes are clustered in the mouse and human genomes (17) suggests that epigenetic mechanisms may be involved.

We demonstrate here that the *mpS2* protein is essential for the differentiation



Fig. 4. Analysis of *mpS2*, *mSP*, and *mITF* RNAs in gastrointestinal tissues of *mpS2*^{+/+}, *mpS2*^{+/-}, and *mpS2*^{-/-} mice. Each lane contained 10 μg of total RNA from the indicated tissue. Blots were successively hybridized with *mpS2* (2), *mSP* (3), and *mITF* (21) ³²P-labeled cDNA probes. The *36B4* probe (1) was used as an internal control.

Fig. 3. Histological analysis of gastric and intestinal tissues in *mpS2*^{+/+} and *mpS2*^{-/-} mice at 5 months of age. **(A)** External appearance and **(B)** section of a fresh stomach and duodenum from *mpS2*^{+/+} [(A), left side] and *mpS2*^{-/-} [(A), right side] and *mpS2*^{-/-} [(A), left side and (B)] mice; arrowheads indicate the antropyloric adenoma. **(C)** Glands (G) and pits (P) of an *mpS2*^{+/+} antral section, each occupying approximately one-half of the mucosal thickness. **(D)** An *mpS2*^{-/-} antral section showing, at the periphery of an adenoma, severe hyperplasia and elongated pits. **(E)** Differentiated epithelial cells lining the pits of the normal mucosa. **(F)** An *mpS2*^{-/-} antral section showing high-grade dysplasia of epithelial cells lining the pits. **(G)** and **(H)** *mpS2* immunostaining with Ab502 (24) of paraffin-embedded antral sections from *mpS2*^{+/+} (G) and *mpS2*^{-/-} (H) mice, respectively, showing the absence of *mpS2* protein in *mpS2*^{-/-} mice. **(I)** and **(J)** PAS staining of antral sections from *mpS2*^{+/+} (I) and *mpS2*^{-/-} (J) mice, showing the dramatic decrease of mucus synthesis in *mpS2*^{-/-} mice. **(K)** Intraepithelial carcinoma (delineated by arrowheads) within an adenoma, showing back-to-back growth of glands without intervening stroma. **(L)** Intramucosal carcinoma showing small sheets of epithelial cells (arrowheads) within the lamina propria



(LP). **(M)** and **(N)** Small intestine sections from *mpS2*^{+/+} (M) and *mpS2*^{-/-} (N) mice. **(O)** *mpS2*^{+/+} villi showing normal cellular infiltrate of the LP. **(P)** Thickened *mpS2*^{-/-} villi with increased intraepithelial and LP lymphoid infiltrate. Sections (C) through (F) and (K) through (P) were stained with hematoxylin and eosin. Scale bars in (A) and (B), 5000 μm; in (C), (D), (M), and (N), 160 μm; in (K), 80 μm; in (E) through (J), (O), and (P), 40 μm; and in (L), 30 μm.

(LP). **(M)** and **(N)** Small intestine sections from *mpS2*^{+/+} (M) and *mpS2*^{-/-} (N) mice. **(O)** *mpS2*^{+/+} villi showing normal cellular infiltrate of the LP. **(P)** Thickened *mpS2*^{-/-} villi with increased intraepithelial and LP lymphoid infiltrate. Sections (C) through (F) and (K) through (P) were stained with hematoxylin and eosin. Scale bars in (A) and (B), 5000 μm; in (C), (D), (M), and (N), 160 μm; in (K), 80 μm; in (E) through (J), (O), and (P), 40 μm; and in (L), 30 μm.

program of the antral and pyloric gastric mucosa cells. Strikingly, all *mpS2*^{-/-} mice developed gastric adenoma, and 30% of them showed carcinoma. Thus, *mpS2* may function as a gastric-specific tumor suppressor gene. However, as only 30% of the *pS2*^{-/-} mice developed carcinomas, the loss of *mpS2* protein on its own is clearly not sufficient for malignancy. Additional genetic alteration may be required, as is the case for human colorectal tumorigenesis (18). Interestingly, whereas normal gastric tissues express large amounts of *hpS2*, about 50% of human gastric carcinomas have lost expression of *hpS2* (7, 8, 12, 19). No major alterations in *hpS2* have been found in genomic DNA extracted from gastric carcinomas (19). However, the presence of aberrant *hpS2* transcripts has been reported (7), which suggests that subtle *hpS2* gene modifications (such as mutations leading to aberrant splicing events) might exist in some stomach carcinomas.

striction site; RH2: 5'-ccatcgatagatctGCCACAATTATCCTCTC-3', containing Cla I and Egl II restriction sites; RH3: 5'-agatcgatggatccATGGCCATCGAGAACAC-3', containing Cla I and Bam HI restriction sites; RH4: 5'-ataggtacctctagaGGTGTGTATGTAGCAGG-3', containing Kpn I and Xba I restriction sites. The P1 probe (0.36 kb) was generated by polymerase chain reaction (PCR) with the use of a 5' pBS primer and the 5'-TCAGCACACTGCTCACA-3' (RH5) *mpS2* primer; the P2 probe (0.3 kb) was a Pml I-Bam HI *mpS2* fragment; and the *mITF* probe (420 bp) was isolated by reverse transcriptase PCR from mouse intestine RNA, with the use of the 5'-CCTGTGCAGTGGTCCTGAAGC-3' and 5'-AGCAATCAGATCAGCCTTGTG-3' primers, derived from the *mITF* cDNA sequence (16).

22. A. Gossler, T. Doetschman, R. Korn, *Proc. Natl. Acad. Sci. U.S.A.* **83**, 9065 (1986); T. Lufkin, A. Dierich, M. LeMeur, *Cell* **65**, 1105 (1991).
23. Total RNA was prepared from tissues frozen with

liquid nitrogen, fractionated by agarose gel electrophoresis (1%) in the presence of formaldehyde, and transferred to nylon membranes (Hybond N; Amersham). P. Chomczynski and N. Sacchi, *Anal. Biochem.* **162**, 156 (1987).

24. The Ab502 polyclonal antibody is directed against a 30-amino acid synthetic peptide corresponding to the COOH-terminal half of *mpS2*.
25. Supported by INSERM; CNRS; Centre Hospitalier Universitaire Régional; Mutuelle Générale de l'Enseignement National; Association pour la Recherche contre le Cancer; the Ligue Nationale Française contre le Cancer and Comité du Haut-Rhin, Fondation pour la Recherche Médicale Française, Fondation de France; and by a grant to P.C. from the Fondation Jeantet. O.L. is the recipient of an IPSEN Foundation fellowship.

13 May 1996; accepted 7 August 1996

Impaired Defense of Intestinal Mucosa in Mice Lacking Intestinal Trefoil Factor

Hiroshi Mashimo, Deng-Chyang Wu, Daniel K. Podolsky,*
Mark C. Fishman

REFERENCES AND NOTES

1. P. Masiakowski *et al.*, *Nucleic Acids Res.* **10**, 7895 (1982).
2. O. Lefebvre *et al.*, *J. Cell Biol.* **122**, 191 (1993).
3. C. Tomasetto *et al.*, *EMBO J.* **9**, 407 (1990).
4. M. Gajhede *et al.*, *Structure* **1**, 253 (1993); A. De *et al.*, *Proc. Natl. Acad. Sci. U.S.A.* **91**, 1084 (1994).
5. M. C. Rio *et al.*, *Science* **241**, 705 (1988); M. C. Rio *et al.*, *C. R. Acad. Sci. Paris* **307**, 825 (1988).
6. N. Wright *et al.*, *J. Pathol.* **162**, 279 (1990); M. C. Rio *et al.*, *Gastroenterology* **100**, 375 (1991).
7. B. Theisinger *et al.*, *Eur. J. Cancer* **27**, 770 (1991).
8. J. A. Henry *et al.*, *Br. J. Cancer* **64**, 677 (1991); C. Welter *et al.*, *Lab. Invest.* **66**, 187 (1992).
9. M. C. Rio and P. Chambon, *Cancer Cells* **2**, 269 (1990).
10. W. Hoffmann and F. Hauser, *Trends Biol. Sci.* **18**, 239 (1993); L. Thim, *Digestion* **55**, 353 (1994).
11. An *mpS2* cDNA probe (2) was used to isolate a 37-kb cosmid containing the *mpS2* gene from a 129/Svj D3 ES cell genomic library (J. M. Garnier, Institut de Génétique et de Biologie Moléculaire et Cellulaire). A 7.1-kb Bam HI fragment containing the whole *mpS2* gene was subcloned into pBluescript II SK+ (pBS) and sequenced.
12. O. Lefebvre *et al.*, data not shown.
13. R. H. Riddell *et al.*, *Hum. Pathol.* **14**, 931 (1983); R. C. Haggitt, *ibid.* **25**, 982 (1994). J. Rosai, *Ackerman's Surg. Pathol.* **8**, 632 (1996).
14. A. Panja, A. Barone, L. Mayer, *J. Exp. Med.* **179**, 943 (1994); B. Rocha, D. Guy-Grand, P. Vassalli, *Curr. Opin. Immunol.* **7**, 235 (1995).
15. R. J. Playford *et al.*, *Proc. Natl. Acad. Sci. U.S.A.* **93**, 2137 (1996).
16. S. Suemori, K. Lynch-Devaney, D. K. Podolsky, *ibid.* **88**, 11017 (1991); M. Tomita *et al.*, *Biochem. J.* **311**, 293 (1995).
17. C. Tomasetto, N. Rockel, M. G. Mattéi, *Genomics* **13**, 1328 (1992); O. Lefebvre, unpublished results.
18. R. A. Weinberg, *Science* **254**, 1138 (1991); S. W. Lee, C. Tomasetto, R. Sager, *Proc. Natl. Acad. Sci. U.S.A.* **88**, 2825 (1991); B. Vogelstein and W. Kinzler, *Trends Genet.* **9**, 138 (1993); A. G. Knudson, *Proc. Natl. Acad. Sci. U.S.A.* **90**, 10914 (1993); R. A. Weinberg, *Cell* **85**, 457 (1996).
19. Y. Luqmani *et al.*, *Int. J. Cancer* **44**, 806 (1989).
20. M. R. Ponce and J. L. Micol, *Nucleic Acids Res.* **20**, 623 (1992).
21. The primers used were as follows (lowercase letters indicate restriction site; uppercase letters indicate *mpS2*-specific sequence). RH1: 5'-ctggatccttagatCATCTGTGTGTTTGGATGC-3', containing a Kpn I re-

The mechanisms that maintain the epithelial integrity of the gastrointestinal tract remain largely undefined. The gene encoding intestinal trefoil factor (ITF), a protein secreted throughout the small intestine and colon, was rendered nonfunctional in mice by targeted disruption. Mice lacking ITF had impaired mucosal healing and died from extensive colitis after oral administration of dextran sulfate sodium, an agent that causes mild epithelial injury in wild-type mice. ITF-deficient mice manifested poor epithelial regeneration after injury. These findings reveal a central role for ITF in the maintenance and repair of the intestinal mucosa.

The gastrointestinal mucosa must maintain a barrier against the harsh luminal contents of acid, enzymes, bacteria, and toxins. Disruption of this barrier is the salient feature of a variety of common and important gastrointestinal disorders, including inflammatory bowel disease and peptic ulcers. Although general protective factors are thought to contribute to this barrier function, the role of specific mucosal surface proteins in sustaining mucosal integrity has not been defined.

The trefoil proteins are a family of proteins expressed specifically and abundantly at the mucosal surface of the gastrointestinal tract (1). They share a distinctive three-leafed secondary structure formed by intrachain disulfide bonds. These proteins appear to resist degradation by proteolytic enzymes and extremes of pH (2). Enhanced expression of trefoil proteins is observed after injury in both the proximal and distal

gastrointestinal tract (3). These proteins are secreted onto the mucosal surface by goblet cells, and in vitro studies suggest that these proteins may promote maintenance of mucosal integrity. Addition of trefoil proteins to wounded intestinal epithelial monolayers increases the rate of restitution, the critical first phase of wound healing in which epithelial continuity is reestablished (4).

To explore the function of trefoil proteins in vivo, we produced mice unable to express ITF, one of the members of this protein family. We used rat ITF cDNA as a probe to isolate the murine *Itf* gene from a phage genomic library, and the identity of this gene was confirmed by nucleotide sequencing (5). A targeting vector for disrupting the gene by homologous recombination in embryonic stem (ES) cells was designed and constructed (Fig. 1A). This targeting vector replaces the entire second exon encoding the trefoil domain with the neomycin resistance gene and abolishes the ability of any resultant peptides to produce the loop structure characteristic of the trefoil proteins. Two independent lines of mice were generated from distinct ES cell clones. Disruption of the *Itf* gene in these mice was confirmed by Southern (DNA) blot analysis and the polymerase chain re-

H. Mashimo, D.-C. Wu, D. K. Podolsky, Gastrointestinal Unit and Center for the Study of Inflammatory Bowel Disease, Jackson 7, Massachusetts General Hospital, Fruit Street, Boston, MA 02114, USA.
M. C. Fishman, Cardiovascular Research Center, Massachusetts General Hospital East, 149 13th Street, Charlestown, MA 02129, USA.

* To whom correspondence should be addressed.